

The energetic and structural properties of bcc NiCu, FeCu alloys: a first-principles study

Yao-Ping Xie and Shi-Jin Zhao

*Institute of Materials Science, School of Materials Science and Engineering,
Shanghai University, Shanghai, 200444, China*

(Dated: January 12, 2013)

Abstract

Using special quasirandom structures (SQS's), we perform first-principles calculations studying the metastable bcc NiCu and FeCu alloys which occur in Fe-Cu-Ni alloy steels as precipitated second phase. The mixing enthalpies, density of state, and equilibrium lattice parameters of these alloys are reported. The results show that quasi-chemical approach and Vegard rule can well predict the energetic and structural properties of FeCu alloys but fail to yield that of NiCu. The reason rests with the difference of bond energy variation with composition between NiCu and FeCu alloys induced by competition between ferromagnetic and paramagnetic state. Furthermore, the calculated results show that the energetic and structural properties of these alloys can well explain the local composition of the corresponding precipitates in ferrite steels.

PACS numbers: 64.60.My, 61.43.Bn, 64.75.Op, 71.20.Be

I. INTRODUCTION

The transitional metals and their alloys related to the magnetism attract much scientific interests. Enormous experimental and theoretical investigations were dedicated to deeper understanding of the nature of their properties which became complicated due to magnetism. Examples of these systems can be provided by artificial crystalline structures fabricated by film growth techniques and precipitated second phase in matrix. Specially, many important properties of materials, such as their mechanical strength, toughness, creep, corrosion resistance, and magnetic properties are essentially controlled by precipitated particles of a second phase. Therefore, understanding of these alloys is also desirable from the views of applications.

The Cu-rich precipitates, which are commonly found in alloy steels, have good strengthening effect on steels. The high-strength low-alloy steels strengthened by copper rich precipitates also retain the impact toughness, corrosion resistance, and welding properties[1–6]. However, it is also confirmed that the presence of Cu-rich precipitates in reactor pressure vessel(RPV) steels is the origin of embrittlement [7], which limit the reactor operating life. The embrittlement effect can be enhanced by the content of Cu or Ni of alloyed steels containing of both Cu and Ni[8–12]. Thus, the mechanism of strengthening and embrittlement of Cu precipitates attract much interest[13–22]. The structure and composition of precipitated phase also became important, and it had been studied by many experiments, such as atom probe field ion microscopy(APFIM) [23–25], small-angle neutron scattering(SANS) [26], high-resolution and conventional electron microscopy(HREM and CTEM) [27, 28], etc. It was observed that small Cu-rich precipitates with diameters less than about 5 nm have a meta-stable body-centered cubic (bcc) structure and are coherent with the α -Fe matrix [26–28] in the initial stage of segregation. In addition, it was also found that Ni also occurs in the Cu-rich precipitates beside Cu and Fe. For HSLA steels, Ni was observed at the coherent matrix/Cu-precipitate heterophase interfaces [29, 30, 36, 37]. For RPV steels, it was also observed Ni appeared in the Cu-rich precipitates at very initial stage and was rejected from the core with the precipitates growth[21, 22, 33, 34].

The bcc FeCu alloy has been studied intensively by theoretical investigations for well understanding of precipitated phase. First-principles calculations based on the cluster expansion framework gave the composition range of mechanical stability of FeCu random

alloy[35]. A thermodynamic equilibrium analysis was used to investigate the composition dependence of Gibbs energy of FeCu alloy as well as the interfacial energy between precipitates and matrix[36]. In the meanwhile, the vibrational energies of dilute FeCu alloys were investigated by first-principles calculations in combination with thermodynamical modeling, which show that the vibrational energies can stabilize the alloys [37]. The dependence of magnetism on the structural characteristics of Cu nucleation and the electronic structure for bcc $\text{Fe}_x\text{Cu}_{1-x}$ ($x > 0.75$) systems were also well investigated[38]. However few systematic investigation of bcc NiCu alloys was reported. The bcc NiCu, like bcc FeCu, is not only a typical system related to magnetism in solids, but also became interesting because of its important contribution to strengthening and embrittlement of the ferrite steels. Therefore, systematic investigations of their properties at electronic level have both foundational and engineering significance. In this paper, the composition-dependent bcc $\text{Ni}_x\text{Cu}_{1-x}$ and $\text{Fe}_x\text{Cu}_{1-x}$ random alloys are investigated by employing special quasi-random structures (SQS's) in the frame of first-principles calculations.

II. MODELING AND THEORETICAL METHODS

The SQS method was proposed by Zunger and Wei et al to overcome the limitations of mean-field theories [41, 42], without the prohibitive computational cost associated with directly constructing large super cells with random occupy of atoms. The SQS method was extensively used to study the properties of semiconductor alloys which are all fcc-based system. Recently, this method was also used into both fcc and bcc transition metal systems and was proved to be useful [43, 44]. For a binary substitutional alloy, many properties are dependent on its configuration. A binary AB substitutional alloy with a lattice of N sites has 2^N possible atomic arrangements, denoted as configurations σ . The measurable property $\langle E \rangle$ represents an ensemble average over all 2^N configuration σ , $\langle E \rangle = \sum \rho(\sigma)E(\sigma)$. The structure σ can be discretized into its component figure f , which is characterized by a set of correlation functions $\bar{\Pi}_{k,m}$. Therefore, $\langle E \rangle$ can be rewrite as $\langle E \rangle = \sum \bar{\Pi}_{k,m}\varepsilon(f)$. The SQS's are special designed N atoms periodic structures whose distinct correlation functions $\bar{\Pi}_{k,m}$ best match ensemble averaged $\langle \bar{\Pi}_{k,m} \rangle$ of random alloys.

The choice of SQS's are critical for the calculations[45]. In this paper, SQS's containing 32 atoms are constructed for bcc alloys, which are shown in Fig. 1. The vectors of lattice are

$\vec{a}_1 = (1.0, -2.0, 0.0)a_0$, $\vec{a}_2 = (0.0, -4.0, 2.0)a_0$, $\vec{a}_3 = (-2.0, 0.0, -2.0)a_0$, respectively, and a_0 is the lattice parameter of the bcc unit cell. The occupations of these sites for the SQS's at $x = 0.25$ and $x = 0.5$ are given in Table 1, and their structural correlations function $\bar{\Pi}_{k,m}$ compared with ideal random alloy correlation functions are given in Table 2. As can be seen, the quality of the SQS's used in these calculation is reasonably good.

First-principles calculations are performed using the density functional theory[46–48] as implemented in the Vienna ab initio simulation package(VASP)[49]. The generalized gradient approximation(GGA)[50, 51] is used for the exchange correlation functional. The interaction between core and valence electrons is described with the projector augmented wave (PAW) potential [52, 53]. The equilibrium structures were determined, up to a precision of 10^{-4} eV in total-energy difference and with a criterion that required the force on each atom to be less than 0.01 eV/Å in atomic forces. The convergence tests with k-point and energy cutoff are presented in table 3. The k-point meshes $6 \times 2 \times 4$ for the Brillouin zone integration are used for SQS's, which is equivalent k-point sampling with Monkhorst-Pack mesh $11 \times 11 \times 11$ for bcc primitive cell. An energy cutoff of 280 eV is applied in all cases.

III. RESULTS AND DISCUSSIONS

Firstly, basic properties of bcc Fe, Ni, Cu are presented. The lattice constant and the magnetic moment for bcc Fe at the equilibrium volume are 2.83 Å and $2.16 \mu_B/\text{atom}$, respectively. The lattice constant and bulk modulus for bcc Cu at the equilibrium volume are 2.89 Å and 130 GPa. These results are in agreement with earlier studies[35, 39]. The magnetic moment for bcc Ni at the equilibrium structure with lattice of 2.81 Å is $0.55 \mu_B/\text{atom}$. The calculated result is well consistent with previous works using GGA, which predicted bcc Ni is ferromagnetic[54, 55]. Previous theoretical works using local density approximation (LDA) predicted bcc Ni is paramagnetic[39]. However, it is confirmed that bcc Ni do possesses a magnetic moment of $0.52 \mu_B/\text{atom}$ by experiments more recently[56]. In addition, it was proved that the GGA calculations can describe satisfactorily lattice and elastic constants of Ni in their observed structures[55].

The mixing enthalpies(ΔH) of bcc NiCu and FeCu random alloys obtained by first-principles SQS method are shown in Fig .2. The mixing enthalpy is heat quantity absorbed(or evolved) during mixing two elements to make homogeneous solid solution, which

is defined as:

$$\Delta H = E_{AB} - xE_A - (1 - x)E_B \quad (1)$$

where E_A , E_B , and E_{AB} are the total energy of A, B, and AB alloy, and x is the composition of alloys. In the frame of quasi-chemical approach[57], the mixing enthalpy is only determined by the composition-independent bond energy between adjacent atoms. Hence, mixing enthalpy can be written as:

$$\Delta H = \Omega x(1 - x), \quad (2)$$

where $\Omega = N_a z (\varepsilon_{A-B} - \frac{1}{2}(\varepsilon_{A-A} + \varepsilon_{B-B}))$ is interaction parameter, N_a is Avogadro's number, ε is bond energy, and z is the number of bonds per atom. Thus, the composition-independent bond energy between atoms would result a parabolic variation for mixing enthalpies with compositions. It can be seen from Fig. 2, the variation of mixing enthalpies of FeCu with composition is parabolic, while that of mixing enthalpies of NiCu exhibit a strong asymmetry and change sign as function of concentration. These effect were also found for random fcc NiCu alloys in previous calculations[40].

To study the effect of degree of disorder on the mixing enthalpies of NiCu, we calculate the ordered structures comparing disordered structures. Three 4-atoms-super-cells are used to simulate order alloys with composition $x = 0.25, 0.50, 0.75$. The mixing enthalpies of these order alloys are represented by solid squares in Fig. 2(a). It shows the mixing enthalpies of this ordered structures of NiCu are all lower than those of disordered alloy with the same extent, and the trend of mixing enthalpies variations with compositions are the same as that of disorder alloys. The mixing enthalpies of order alloy also exhibit a strong asymmetry. Therefore, the degree of disorder is not the reason of the asymmetry of mixing enthalpies for NiCu alloys.

We turn to investigate bonding property of NiCu and FeCu from electronic structures for understanding strong asymmetry variation of mixing enthalpies with composition. The bond energy is critical factor that determines the mixing enthalpies. The variation of the bond energy can be reveal from comparison of the density of states(DOS) of $\text{Fe}_x\text{Cu}_{1-x}$ and $\text{Ni}_x\text{Cu}_{1-x}$. Since the bond energies of transitional metal are determined by the coupling of d-band, the d-bands of Cu, Fe, Ni in $\text{Fe}_x\text{Cu}_{1-x}$ and $\text{Ni}_x\text{Cu}_{1-x}$ with different compositions are plotted in Fig 3. One can easily understand the difference of mixing enthalpies magnitude between FeCu and NiCu from electronic structure. In comparison with the occupation of

Ni, the occupation of Fe in the alloy is changed significantly from that of pure Fe (see DOS around 2 eV in Fig. 3). Therefore, the energy of Fe-Cu bond is much larger than that of Ni-Cu bond, and the mixing enthalpies of CuFe are much larger than those of CuNi. Furthermore, bond energies in alloys vary with compositions can be also reflected by the DOS. The DOS peaks of Ni vary with composition, while that of Fe in alloys with different compositions are the same. These findings indicate that bond energy ε of Ni-Cu varies with composition. It can be known from equation (2), the variation of bond energy induce composition-dependent interaction parameter Ω , which result that the variation of mixing enthalpy with composition is not parabolic. These are consistent with calculated results in Fig 2(a). Hence, the complex variation trend of mixing enthalpies of NiCu derive from the composition-dependent bond energy.

In addition, one can infer that the magnetic moment of Ni atom varies with the composition and the magnetic moment of $\text{Ni}_{0.25}\text{Cu}_{0.75}$ disappears. A more clear presentation of magnetic moment of alloys with different composition is given in Fig. 4. These phenomena can be well understand by using stoner criterion which succeeds in explaining the magnetic property of transitional metal alloys dictated by the filling of the d-band[39]. The Stoner criterion states that ferromagnetism appears when the gain in exchange energy is larger than the loss in kinetic energy. Therefore, there is always a competition between ferromagnetic(FM) and paramagnetic(PM) solutions, and magnetic properties are determined by the state which has lowest energy. The DOS at the Fermi level is a key factor to affect the competition between FM and PM state. A larger peak of DOS at Fermi level induces a larger exchange energy and prefers to split into FM state. Fig. 5 illustrates the unpolarized DOS of NiCu and FeCu alloys. It is shown in Fig. 4 and Fig. 5, the trend of magnetic moment of the system well consistent with the variation of DOS at Fermi level.

For these alloys, the d electrons increase with the Cu concentration, which result the Fermi level of Ni(Fe) be promoted. The key point is, as shown in Fig. 5, since the DOS at Fermi level of NiCu is much smaller than that of FeCu, the Fermi level of NiCu change much rapidly with Cu concentration than that of FeCu which induce that the peak of DOS of NiCu is much sensitive to the alloy composition than that FeCu. Hence, the magnetic moment of Ni change with the variation of DOS at Fermi level when the Cu concentration is changed, and it disappears when the DOS at the Fermi level is 0. Now, we can conclude that the strong asymmetry of mixing enthalpies of NiCu with composition is induced by

band shift because of the competition between FM and PM state.

It is found that the composition-dependent electronic interactions of NiCu alloys also affect the structural property. As shown in Fig. 6, the calculated volume per atom of FeCu alloy well obeys the Vegard law, while that of NiCu deviates from what the Vegard law predicts. According to the Vegard law[58], the lattice constant has a linear relationship with its composition, i.e. $a(A_xB_{1-x}) = xa(A) + (1-x)a(B)$. This implies that the atom can be considered as rigid body whose volume is unchanged with its chemical environment. However, the composition-dependent electronic interaction in NiCu results in the atomic volumes depending on its composition, which induces a bowing effect.

As shown in Fig. 7, the partial atomic pair correlation functions give more detailed information of the alloy structures. It can show that how large is the degree of distortion of equilibrium alloy structure from the perfect bcc structure. For bcc structure, the numbers of 1st, 2nd, 3rd, 4th, 5th neighbors are 8, 6, 12, 24, 8. As is shown in Fig. 7, both NiCu and FeCu alloys are still bcc structure and the lattice just has a minor change, but the NiCu alloy is more close to a perfect bcc structure. Since the nominal number of minority d-band holes of Fe is more than that of Ni by 2 electrons, the partial charge effect of Fe from Cu is stronger than that of Ni. The bond length can be affected by partial charge. Hence, the distance between atomic neighbors of FeCu is more sensitive to their chemical environment than NiCu, which induces a larger distortion of FeCu from bcc.

The strain effect is also very important for the precipitated phase in ferrite matrix. We have calculated the strain energy with lattice constant from 2.80 Å to 2.90 Å as shown in Fig. 8, which covers the lattice constant range of bcc Fe and Cu. It is shown that NiCu alloys have smaller strain energy at lattice of bcc Fe, while FeCu alloys have smaller strain energy at lattice of bcc Cu. At a lattice constant of Fe matrix with 2.83 Å, the strain energies are 6.52, 0.78, 0.51 meV/atom for Ni_xCu_{1-x} ($x=0.25, 0.5, 0.75$) alloys, and 20.71, 13.51, 7.13 meV/atom for Fe_xCu_{1-x} ($x=0.25, 0.5, 0.75$). The strain energy of bcc Cu in ferrite matrix is 21.6 meV/atom. These indicate that Ni and Fe can lower the bcc Cu strain energy in ferrite matrix, while Ni is better than Fe in role of reducing strain energy.

From the energetic and structural properties of alloys, the precipitated phase can be well understood. For HSLA steels, it was observed that NiCu alloys at the matrix/precipitates heterophase interfaces area[29]. The calculated results show that the mixing enthalpies of FeCu are positive, which indicate that the FeCu alloys are unstable and Cu atoms prefer

to segregate to form precipitates. The mixing enthalpies of NiCu alloys are negative when Ni concentrations below 30 at. %, indicating that NiCu alloys with lower Ni concentration are energetic favorable. The element of Ni appears in the matrix/precipitates heterophase interfaces area, which is mainly induced the factors relate to strain: i) The volume per atom of NiCu is similar to that of Fe matrix rather than pure Cu, even rather than that of FeCu alloy, and the stain energy can be much lower by Ni. ii) The structure of NiCu is more close to the bcc structure, which induce little mismatch of lattice. These indicate that NiCu alloys in the interface of matrix/precipitate can contribute lower interface energy from reducing shear stress. However, the experimental peak concentration of Ni is about 3 at. % in the Cu-rich precipitates which is lower than the Ni concentration of most favorable NiCu alloy with concentration of 20 at. %. This indicates that the distribution of elements distribution may be affected by the size effects and vibrational entropy in addition. In RPV steels, the Ni in Cu-precipitates be rejected from the core after thermal-aging or neutron-irradiated[33, 34], and the experimental peak concentration of Ni is among 15-20 at. %, which is well consistent the composition of energetic favorable alloys more closed. These indicate that the element distribution of bcc precipitated phase at very initial of segregation stage can be well understood from the energetic and structural properties.

IV. CONCLUSION

In summary, we propose three 32-atom SQS supercells to mimic the pair and multisite correlation functions of random CuFe and NiCu bcc substitutional alloys which occur in Fe-Cu-Ni alloy steels as precipitated second phase. Those SQS's are used to calculate the mixing enthalpies, density of state, and lattice parameters of the metastable random alloys. The results show that quasi-chemical approach and vegard rule can satisfactorily predict the mixing enthalpies and structure parameters of FeCu alloys but fail to accurately yield that of NiCu. As can be obtained from the analysis of electronic structure, the magnetism induced bond energy variation with composition is the reason that quasi-chemical approach and vegard rule fail to predict the properties of NiCu alloys. Furthermore, the calculated results can well explain the previous experimental observation of local composition of coherent Copper-rich precipitates containing Nickel and confirm that segregation of Ni is drove by thermaldynamic and chemical factor. These suggest that the properties of random alloys

have important implications to better understand the multi-component precipitates.

In this work, we present the intrinsic bulk properties of metastable bcc FeCu and NiCu random alloys to understand the structure of Cu-rich precipitates. Since Cu-rich precipitates have important roles on properties of alloy steels, understanding the formation mechanism is highly desirable for altering the properties of steels by controlling Cu-rich precipitates. Further investigation would simulate realistic interface to calculate the interfacial energy of precipitates/matrix and the diffusion properties of Cu and Fe atom affected by Ni shell, which will clarify the role of Nickel on the evolution of the Cu-rich precipitates.

The authors thank G. Xu and Prof. B. X. Zhou for critical discussions. Y. P. Xie also thanks J. H. Yang and Prof. X. G. Gong for insightful discussion. This work is financially supported by National Science Foundation of China (Grant No. 50931003, 51001067), Shanghai Committee of Science and Technology (Grant No. 09520500100) , Shu Guang project (Grant No. 09SG36) supported by Shanghai Municipal Education Commission and Shanghai Education Development Foundation, and Shanghai Leading Academic Discipline Project (S30107). The computations were performed at Ziqiang Supercomputer Center of Shanghai University and Shanghai Supercomputer Center.

-
- [1] M. E. Fine, R. Ramanathan, S. Vaynman and S. P. Bha Mechanical properties and microstructure of weldable high performance low carbon steel containing copper. In International Symposium on Low-Carbon Steels for the 90's, R. I. Asfahani and G. Tither (Eds.), Pittsburgh, Pennsylvania: TMS. 1993, pp. 511-514
 - [2] S. Vaynman, M. E. Fine, G. Ghosh, and S. P. Bhat, Copper precipitation hardened, high-strength, weldable steel. In Materials for The New Millennium, K. P. Chong (Ed.), Washington D.C.: ASCE. 1996, pp. 1551
 - [3] S. Vaynman, I. J. Uslander, and M. E. Fine, High-strength, weldable, air-cooled, copper-precipitation-hardened steel. In 39th Mechanical Working and Steel Processing Conference Proceedings, Indianapolis, Indiana: ISS. 1997, pp. 1183-1190
 - [4] S. Vaynman, and M. E. Fine, High-performance, weatherable, copper-precipitation-hardened steel. In International Symposium on Steel for Fabricated Structures, R. I. Asfahani and R. L. Bodnar (Eds.), Cincinnati, Ohio: AISI and ASM International. 1999, pp. 59-66

- [5] S. Vaynman, M. E. Fine, R. I. Asfahani, D. M. Bormet, and C. Hahin, High performance copper-precipitation-hardened steel. In *Microalloyed Steel*, R. I. Asfahani, R. L. Bodnar and M. J. Merwin (Eds.), Columbus, Ohio: ASM. 2002
- [6] S. Vaynman, M. E. Fine, and S. P. Bhat, High-strength, low-carbon, ferritic, copper-precipitation-strengthened steels for tank car applications. In *Materials Science and Technology*, New Orleans, Louisiana: AIST and TMS, 2004, pp. 417
- [7] Y. Nagai, Z. Tang, M. Hassegawa, T. Kanai and M. Saneyasu, *Phys Rev B* 6313 (13), - (2001).
- [8] P. Efsing, C. Jansson, T. Mager and G. Embring, *ASTM international* 4, 1(2007)
- [9] R. Ahlstrand, M. Bièth and Claude Rieg, *Nuclear Engineering and Design*, 230, 267(2004)
- [10] B. Acostaa, L. Debarberisa, F. Sevinia and A. Kryukov, *NDT E International* 37, 321(2004)
- [11] L. Debarberisa, F. Sevinia, B. Acostaa, A. Kryukovb, Y. Nikolaevb, A.D. Amaevb, M. Valo, *International Journal of Pressure Vessels and Piping* 79, 637(2002)
- [12] J. R. Hawthore, *ASTM-STP* 782, 1982.375
- [13] S. Nedelcu, P. Kizler, S. Schmauder and N. Moldovan, *Model Simul Mater Sc* 8 (2), 181-191 (2000).
- [14] T. Harry and D. J. Bacon, *Acta Mater* 50 (1), 195-208 (2002).
- [15] T. Harry and D. J. Bacon, *Acta Mater* 50 (1), 209-222 (2002).
- [16] C. S. Shin, M. C. Fivel, M. Verdier and K. H. Oh, *Philos Mag* 83 (31-34), 3691-3704 (2003).
- [17] D. J. Bacon and Y. N. Osetsky, *J Nucl Mater* 329-33, 1233-1237 (2004).
- [18] C. Kohler, P. Kizler and S. Schmauder, *Model Simul Mater Sc* 13 (1), 35-45 (2005).
- [19] Z. Z. Chen, N. Kioussis and N. Ghoniem, *Phys Rev B* 80 (18), - (2009).
- [20] A. Takahashi and N. M. Ghoniem, *J Mech Phys Solids* 56 (4), 1534-1553 (2008).
- [21] M. K. Miller and K. F. Russell, *J Nucl Mater* 371 (1-3), 145-160 (2007)
- [22] M. K. Miller, K. F. Russell, M. A. Sokolov and R. K. Nanstad, *J Nucl Mater* 361 (2-3), 248-261 (2007).
- [23] M. K. Miller, K. F. Russell, P. Pareige, M. J. Starink, and R. C. Thompson, *Mater Sci Eng* 250 (1998) 49-54
- [24] N. Murayama, M. Sugiyama, T. Hara, and H. Tamehiro, *Mater Trans JIM*, 40 (1999) 268-277
- [25] M. Murayama, Y. Katayama, and K. Hono, *Metall Trans A* 30 (1999) 345-353
- [26] K. Osamura, H. Okuda, M. Takashima, K. Asano, and M. Furusaka, *Mater Trans JIM* 34 (1993) 305-311

- [27] P. J. Othen, M. L. Jenkins, G. W. D. Smith, and W. J. Phythian. *Philos Mag Lett* 64 (1991) 383-391
- [28] P. J. Othen, M. L. Jenkins, and G. W. D. Smith, *Philos Mag A* 70 (1994) 1-24
- [29] D. Isheim, M. S. Gagliano, M. E. Fine, and D. N. Seidman, *Acta Mater.* 54 (2006) 841-849
- [30] D. Isheim, and D. N. Seidman, *Surf. Interface Anal.* 36 (2004) 569-574
- [31] R. P. Kolli and D. N. Seidman, *Acta Mater* 56 (9), 2073-2088 (2008).
- [32] R. P. Kolli, R. M. Wojes, S. Zaucha and D. N. Seidman, *Int J Mater Res* 99 (5), 513-527 (2008).
- [33] J. M. Hyde, G. Sha, E. A. Marquis, A. Morley, K.B. Wilford, T.J. Williams, *Ultramicroscopy*, (doi:10.1016/j.ultramic.2010.12.030)
- [34] P. J. Pareige, K. F. Russell, M. K. Miller, *Appl. Surf. Sci* 94/95 (1996) 362-369
- [35] J. Z. Liu, A. van de Walle, G. Ghosh, and M. Asta, *Phys. Rev. B* 72 (2005) 144109
- [36] E. Kozeschnik, *Scr. Mater.* 59 (2008) 1018-1021
- [37] D. Reith, and R. Podloucky, *Phys. Rev. B* 80 (2009) 054108
- [38] H. Choi, C. Kim, and Y. C. Chung, *J. Appl. Phys.* 106 (2009) 083910
- [39] P. James, O. Eriksson, B. Johansson and I. A. Abrikosov, *Phys Rev B* 59 (1999) 419
- [40] I. A. Abrikosov, H. L. Skriver, *Phys Rev B* 47 (1993) 16532
- [41] A. Zunger, S. H. Wei, L. G. Ferreira, and J. E. Bernard, *Phys. Rev. Lett.* 65 (1990) 353
- [42] S. H. Wei, L. G. Ferreira, J. E. Bernard, and A. Zunger, *Phys. Rev. B* 42 (1990) 9622
- [43] C. Jiang, C. Wolverton, J. Sofo, L. -Q. Chen, and Z. K. Liu, *Phys. Rev. B* 69 (2004) 214202
- [44] G. Ghosh, A. van de Walle, and M. Asta, *Acta Mater.* 56 (2008) 3202-3221
- [45] A. V. Ruban and I. A. Abrikosov, *Rep. Prog. Phys.* 71 (2008) 046501
- [46] P. Hohenberg, and W. Kohn, *Phys. Rev.* 136 (1964) B864
- [47] W. Kohn, and L. J. Sham, *Phys. Rev.* 140 (1965) A1133
- [48] R. O. Jones, and O. Gunnarsson, *Rev. Mod. Phys.* 61 (1989) 689-746
- [49] G. Kresse, and J. Furthmüller, *Phys. Rev. B* 54(1996) 11169; *Comput. Mater. Sci.* 6 (1996) 15-50
- [50] Y. Wang, and J. P. Perdew, *Phys. Rev. B* 44 (1991) 13298
- [51] J. P. Perdew, J. A. Chevary, S. H. Vosko, K. A. Jackson, M. R. Pederson, D. J. Singh, and C. Fiolhais, *Phys. Rev. B* 46 (1992) 6671
- [52] P. E. Blöchl, *Phys. Rev. B* 50 (1994) 17953

- [53] G. Kresse and D. Joubert, Phys. Rev. B 59 (1999) 1758
- [54] X. He, L. T. Kong, and B. X. Liua, J. Appl. Phys. 97, 106107(2005).
- [55] G. Y. Guo and H. H. Wang, Chin. J. Phys. 38, 949 (2000).
- [56] C. S. Tian, D. Qian, D. Wu, R.H. He, Y. Z. Wu, W.X. Tang, L. F. Yin, Y. S. Shi, G. S. Dong, X. F. Jin, X. M. Jiang, F. Q. Liu, H. J. Qian, K. Sun, L. M. Wang, G. Rossi, Z. Q. Qiu, J. Shi, Phys. Rev. Lett, 94, 137210 (2005)
- [57] D. A. Porter and K. E. Easterling, Phase Transformations in Metals and Alloys, second ed., CRC Press,1992
- [58] L. Vegard, Z. Phys. 5 (1921) 17

TABLE I: Atomic coordinates and occupation of the 32 atoms bcc SQS.

| Atomic coordinates | | | | | | | | | | | | |
|--------------------|------|------|-------|------|------|-------|------|------|-------|------|------|------|
| AB | | | | | | | | | | | | |
| A: | 0.0 | -4.0 | 0.0; | 0.0 | -2.0 | 0.0; | -0.5 | -0.5 | -0.5; | -1.0 | -4.0 | -1.0 |
| A: | -0.5 | -1.5 | -0.5; | 0.0 | -1.0 | 0.0; | -1.0 | -3.0 | -1.0; | 0.5 | -4.5 | 1.5 |
| A: | 0.5 | -5.5 | 1.5; | -1.5 | -2.5 | -0.5; | -1.5 | -3.5 | -0.5; | -0.5 | -2.5 | 0.5 |
| A: | -1.0 | -6.0 | 0.0; | -0.5 | -3.5 | 0.5; | 0.0 | -3.0 | 1.0; | -1.0 | -5.0 | 0.0 |
| B: | -0.5 | -4.5 | 0.5; | -0.5 | -5.5 | 0.5; | 0.0 | -5.0 | 1.0; | 0.5 | -2.5 | 0.5 |
| B: | 0.5 | -3.5 | 0.5; | -1.5 | -0.5 | -1.5; | -1.5 | -1.5 | -1.5; | -1.0 | -1.0 | -1.0 |
| B: | -1.0 | -2.0 | -1.0; | -0.5 | -2.5 | -0.5; | -0.5 | -3.5 | -0.5; | 0.0 | -3.0 | 0.0 |
| B: | 0.0 | -6.0 | 1.0; | 0.0 | -4.0 | 1.0; | -1.0 | -3.0 | 0.0; | -1.0 | -4.0 | 0.0 |
| AB ₃ | | | | | | | | | | | | |
| A: | 0.0 | -2.0 | 0.0; | 0.5 | -2.5 | 0.5; | 0.5 | -3.5 | 0.5; | 0.0 | -1.0 | 0.0 |
| A: | -0.5 | -3.5 | -0.5; | 0.0 | -3.0 | 0.0; | 0.0 | -4.0 | 1.0; | -1.5 | -2.5 | -0.5 |
| B: | 0.0 | -4.0 | 0.0; | -1.5 | -0.5 | -1.5; | -1.5 | -1.5 | -1.5; | -1.0 | -1.0 | -1.0 |
| B: | -0.5 | -0.5 | -0.5; | -1.0 | -4.0 | -1.0; | -1.0 | -2.0 | -1.0; | -0.5 | -1.5 | -0.5 |
| B: | -1.0 | -3.0 | -1.0; | -0.5 | -2.5 | -0.5; | 0.0 | -6.0 | 1.0; | 0.5 | -4.5 | 1.5 |
| B: | 0.5 | -5.5 | 1.5; | -1.5 | -3.5 | -0.5; | -1.0 | -3.0 | 0.0; | -0.5 | -2.5 | 0.5 |
| B: | -1.0 | -6.0 | 0.0; | -1.0 | -4.0 | 0.0; | -0.5 | -3.5 | 0.5; | 0.0 | -3.0 | 1.0 |
| B: | -1.0 | -5.0 | 0.0; | -0.5 | -4.5 | 0.5; | -0.5 | -5.5 | 0.5; | 0.0 | -5.0 | 1.0 |

TABLE II: Comparison of correlation function $\overline{\Pi}_{k,m}$ of 32 atoms bcc SQS and ideal value of random alloy.

| | AB | | AB ₃ | |
|------------------------|--------|------|-----------------|------|
| | random | SQS | random | SQS |
| $\overline{\Pi}_{2,1}$ | 0 | 0 | 0.25 | 0.25 |
| $\overline{\Pi}_{2,2}$ | 0 | 0 | 0.25 | 0.25 |
| $\overline{\Pi}_{2,3}$ | 0 | 0 | 0.25 | 0.25 |
| $\overline{\Pi}_{2,4}$ | 0 | 0 | 0.25 | 0.25 |
| $\overline{\Pi}_{2,5}$ | 0 | 0.17 | 0.25 | 0.04 |
| $\overline{\Pi}_{2,6}$ | 0 | 0 | 0.25 | 0.25 |
| $\overline{\Pi}_{3,2}$ | 0 | 0.03 | 0.13 | 0.13 |
| $\overline{\Pi}_{4,2}$ | 0 | 0 | 0.06 | 0.08 |

TABLE III: Total energies of bcc primitive cell of Fe, Ni and Cu as a function of the number of k points and the cutoff energy.

| Monkhorst-Pack mesh | energy cutoff(eV) | bcc Fe | bcc Cu | bcc Ni |
|--------------------------|-------------------|--------|--------|--------|
| $3 \times 3 \times 3$ | 280 | -8.15 | -4.13 | -5.27 |
| $5 \times 5 \times 5$ | 280 | -8.12 | -3.71 | -5.33 |
| $7 \times 7 \times 7$ | 280 | -8.17 | -3.70 | -5.39 |
| $9 \times 9 \times 9$ | 280 | -8.17 | -3.70 | -5.37 |
| $11 \times 11 \times 11$ | 280 | -8.17 | -3.70 | -5.37 |
| $13 \times 13 \times 13$ | 280 | -8.17 | -3.70 | -5.37 |
| $11 \times 11 \times 11$ | 180 | -6.99 | -1.97 | -4.05 |
| $11 \times 11 \times 11$ | 260 | -8.15 | -3.68 | -5.36 |
| $11 \times 11 \times 11$ | 300 | -8.17 | -3.70 | -5.37 |

(a) (b)

FIG. 1: Crystal structures of the SQS-32 supercell in their unrelaxed forms. Blue and red spheres represent A and B atoms, respectively. (a) AB (b) AB₃

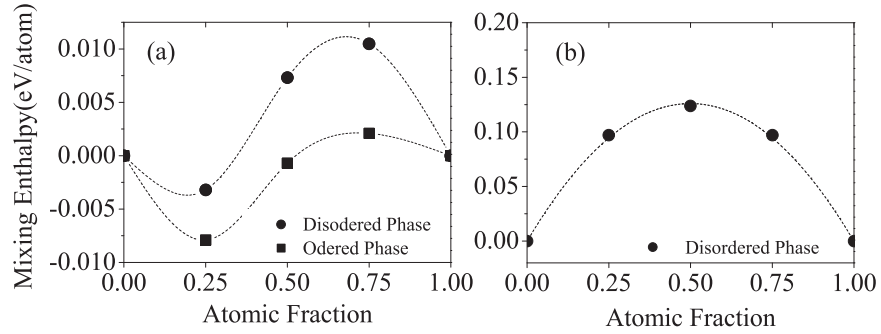


FIG. 2: Mixing enthalpy of alloys: (a) disordered and ordered Ni_xCu_{1-x}, (b) disordered Fe_xCu_{1-x}.

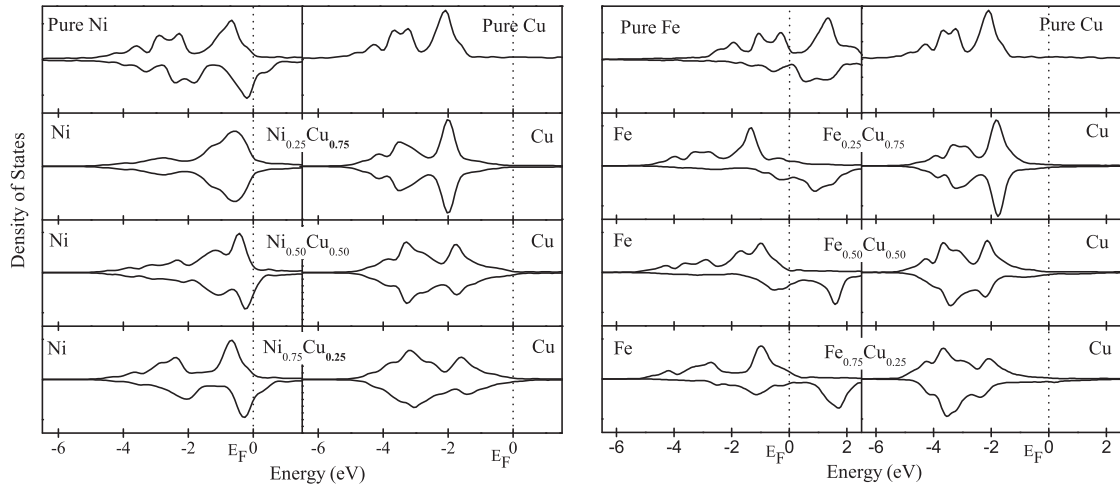


FIG. 3: Comparison of the d-band between pure metals and alloys. The d-band of Ni, Fe, Cu in pure Ni, Fe, Cu, NiCu alloy, FeCu alloy are plot in each panel.

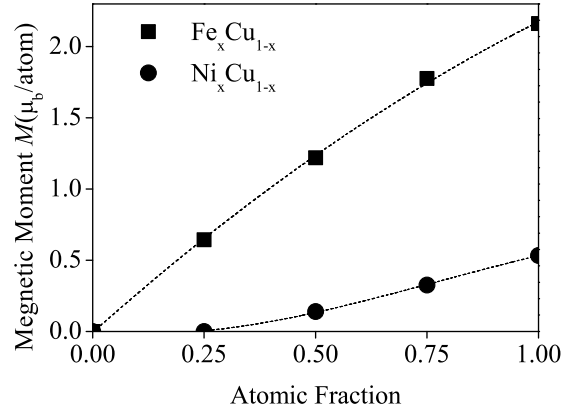


FIG. 4: Magnetic moments per atom in NiCu and FeCu alloys.

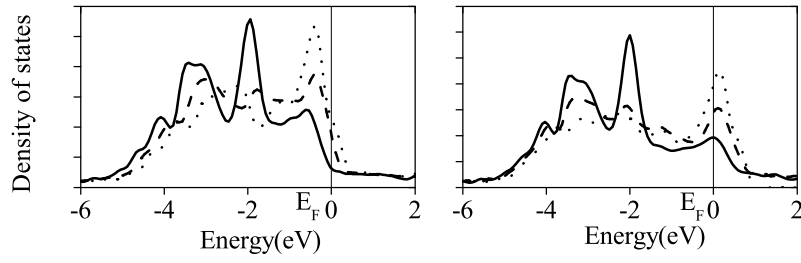


FIG. 5: The unpolarized calculated density of state(DOS) of NiCu and FeCu alloys. The solid, dash, dot line denote for $\text{Ni(Fe)}_x\text{Cu}_{1-x}$, $x = 0.25, 0.50, 0.75$, respectively.

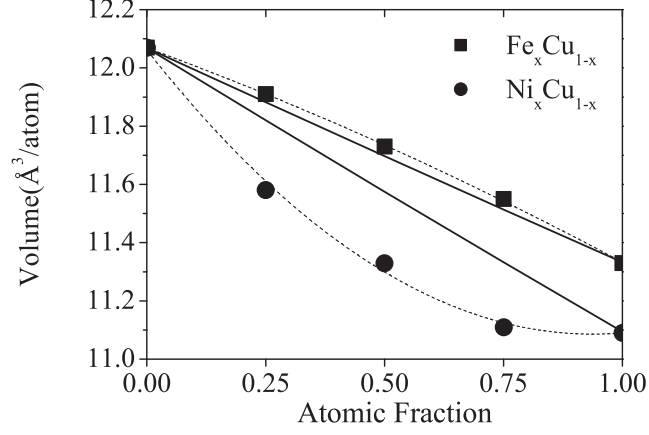


FIG. 6: Atomic volume versus composition in bcc $\text{Ni}_x\text{Cu}_{1-x}$ and $\text{Fe}_x\text{Cu}_{1-x}$ alloys. The circles and squares denote the calculated results of SQS method. The solid lines denote the results predicted by Vegard rule.

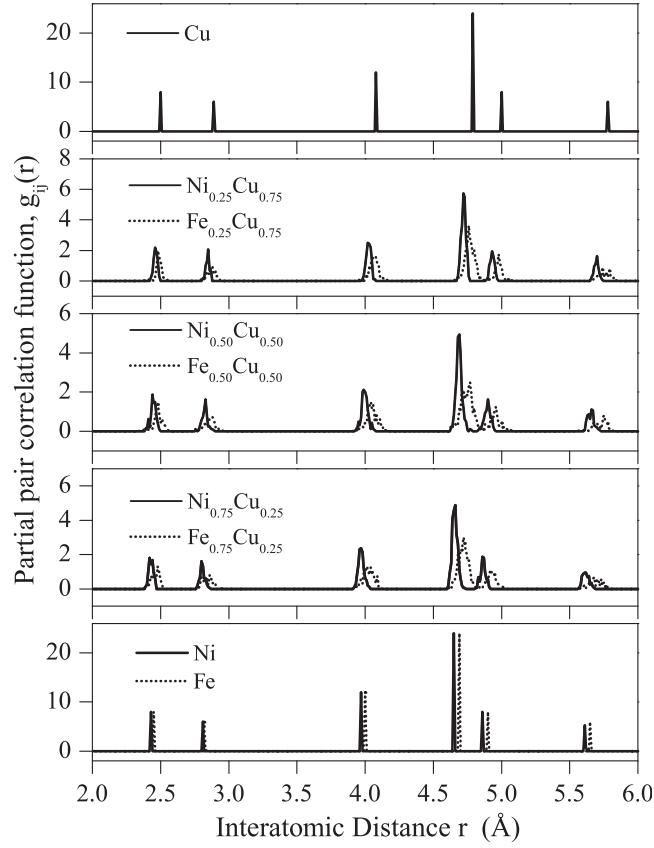


FIG. 7: Partial atomic pair correlation function $g_{ij}(r)$ in NiCu and FeCu alloys.

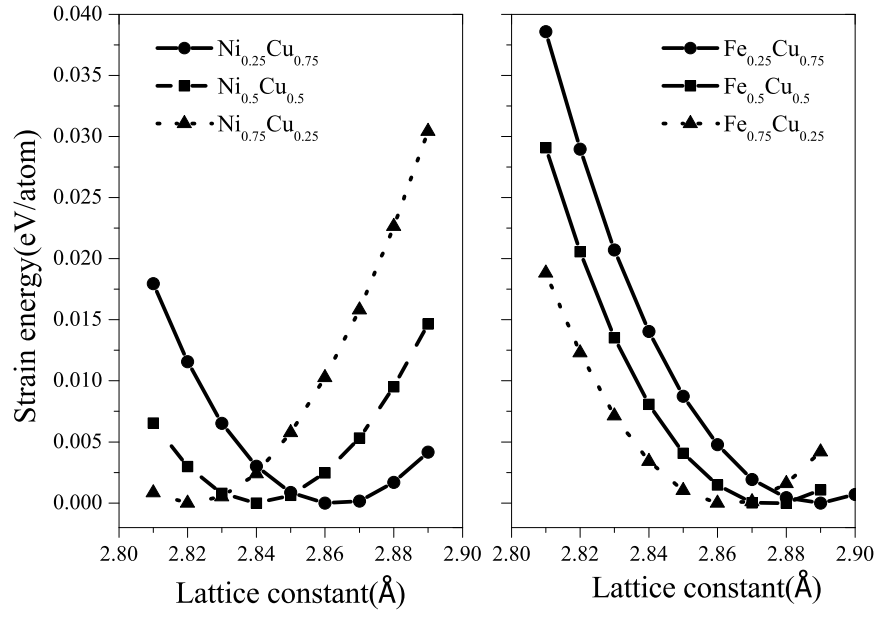


FIG. 8: The strain energy of NiCu and FeCu as a function of lattice constant.